Biochimica et Biophysica Acta 1842 (2014) 677–685

Contents lists available at ScienceDirect

Biochimica et Biophysica Acta

journal homepage: www.elsevier.com/locate/bbadis

Development and pathomechanisms of cardiomyopathy in very long-chain acyl-CoA dehydrogenase deficient (VLCAD$^{-/-}$) mice

Sara Tucci [a,b,*,1], Ulrich Flögel [c,1], Sven Hermann [d], Marga Sturm [b], Michael Schäfers [d], Ute Spiekerkoetter [a]

[a] Department of General Pediatrics, Center for Pediatrics and Adolescent Medicine, University Hospital Freiburg, 79106 Freiburg, Germany
[b] Department of General Pediatrics, University Children's Hospital Duesseldorf, 40225 Duesseldorf, Germany
[c] Department of Molecular Cardiology, Heinrich Heine University Duesseldorf, 40225 Duesseldorf, Germany
[d] European Institute for Molecular Imaging — EIMI, University of Muenster, 48149 Muenster, Germany

ARTICLE INFO

Article history:
Received 11 December 2013
Received in revised form 15 January 2014
Accepted 4 February 2014
Available online 12 February 2014

Keywords:
VLCAD-deficiency
Dilated cardiomyopathy
MRI
PET
MCT-supplementation
Energy metabolism

ABSTRACT

Hypertrophic cardiomyopathy is a typical manifestation of very long-chain acyl-CoA dehydrogenase deficiency (VLCADD), the most common long-chain β-oxidation defects in humans; however in some patients cardiac function is fully compensated. Cardiomyopathy may also be reversed by supplementation of medium-chain triglycerides (MCT). We here characterize cardiac function of VLCAD-deficient (VLCAD$^{-/-}$) mice over one year. Furthermore, we investigate the long-term effect of a continuous MCT diet on the cardiac phenotype. We assessed cardiac morphology and function in VLCAD$^{-/-}$ mice by in vivo MRI. Cardiac energetics were measured by ^{31}P-MRS and myocardial glucose uptake was quantified by positron-emission-tomography (PET). Metabolic adaptations were identified by the expression of genes regulating glucose and lipid metabolism using real-time-PCR. VLCAD$^{-/-}$ mice showed a progressive decrease in heart function over 12 months accompanied by a reduced phosphocreatine-to-ATP-ratio indicative of chronic energy deficiency. Long-term MCT supplementation aggravated the cardiac phenotype into dilated cardiomyopathy with features similar to diabetic heart disease. Cardiac energy production and function in mice with a β-oxidation defect cannot be maintained with age. Compensatory mechanisms are insufficient to preserve the cardiac energy state over time. However, energy deficiency by impaired β-oxidation and long-term MCT induce cardiomyopathy by different mechanisms. Cardiac MRI and MRS may be excellent tools to assess minor changes in cardiac function and energetics in patients with β-oxidation defects for preventive therapy.

1. Introduction

Hypertrophic cardiomyopathy and arrhythmias are typical manifestations of the severe early-onset phenotype of very-long-chain acyl-CoA dehydrogenase deficiency (VLCADD) [1], the most common disorder of the mitochondrial long-chain fatty acid oxidation (mFAO) pathway [2]. Especially in situations of increased energy demand, VLCAD-deficient patients may undergo severe metabolic derangement leading to life-threatening events, coma and death [3]. The recommended treatment includes supplementation with medium-chain triglycerides (MCT) as partial or complete replacement of the normal long-chain triglycerides (LCT) [4,5]. Medium-chain fatty acids easily by-pass the first step of the mFAO catalyzed by VLCAD and may be fully metabolized for energy production. The supplementation with MCT can completely reverse acute hypertrophic cardiomyopathy in affected patients [6,7]. However, a continuous MCT diet in asymptomatic patients is widely debated.

The implementation of neonatal screening for VLCADD allowed the identification of an ever increasing number of patients and contributed significantly to an improvement in disease morbidity and mortality. In fact, some patients remain asymptomatic over long periods of time also without preventive measures that are usually initiated after positive screening. Thus, the heart seems to be able to compensate for a defective mFAO by alternative mechanisms of energy production. Whether these compensatory mechanisms can persist and maintain their efficiency life-long is arguable. To gain insights into the long-term fate of VLCADD, we explored VLCAD-deficient (VLCAD$^{-/-}$) mice [8] presenting with a similar clinical phenotype as humans [9–14]. However, in contrast to humans mice also express an enzyme with overlapping substrate specificity, the long-chain acyl-CoA dehydrogenase (LCAD). This enzyme has also been described to play an important role in the murine mFAO pathway especially for the oxidation of long-

* Corresponding author at: Department of General Pediatrics, Center for Pediatrics and Adolescent Medicine, University Hospital, Mathildenstrasse 1, 79106 Freiburg, Germany. Tel.: +49 761 270 43700; fax: +49 761 270 45270.
E-mail address: sara.tucci@uniklinik-freiburg.de (S. Tucci).
[1] Equally contributed.

http://dx.doi.org/10.1016/j.bbadis.2014.02.001
0925-4439/

chain unsaturated fatty acids [15]. In particular, the LCAD knockout mouse model accumulates the same acylcarnitine species as occur in VLCADD patients and present with a prominent cardiac hypertrophy at birth [16].

With regard to the heart, VLCAD$^{-/-}$ mice have been reported to display an altered calcium homeostasis [17], prolonged QT interval [18] as well as a mild hypertrophy at three months of age [19] while they are fully asymptomatic at birth although lacking the complete *Acadvl* gene. These characteristics make VLCAD$^{-/-}$ mice an excellent model for the investigation of pathomechanisms involved in the development of symptoms caused by the lack of VLCAD long-term. Since follow-up studies of the cardiac phenotype in adults are still missing and the chronic effects of a defective mFAO machinery on cardiac function and morphology are still unknown we monitored cardiac function in vivo over a period of one year by cine-MRI. In VLCAD$^{-/-}$ mice cardiac energetics were determined by in vivo 2D ^{31}P chemical shift imaging (CSI) and myocardial glucose uptake was studied by positron-emission tomography (PET). Metabolic adaptations under normal and long-term MCT diet were investigated by analysis of genes regulating cardiac glucose and lipid metabolism. Furthermore, cardiac lipid accumulation, markers of oxidative stress as well as the reactivation of the fetal gene program were examined.

2. Materials and methods

2.1. Animals

Experiments were performed on fourth- to fifth-generation intercrosses of C57BL6 + 129sv VLCAD genotypes. Littermates served as controls and genotyping of mice was performed as described previously in Exil et al. [8]. Groups consisting of 10–12 mice, at the age of three, six and 12 months were investigated under well-fed conditions. After the final examination, the mice were sacrificed by CO_2 asphyxiation and the heart was rapidly removed and immediately frozen in liquid nitrogen.

All animal studies were performed with the approval of the Heinrich Heine University Institutional Animal Care and Use Committee and in accordance with the Committees' guidelines (Landesamt für Natur, Umwelt und Verbraucherschutz, LANUV, Germany; file number: 8.87-50.10.34.09.072).

2.2. Diet composition and supplementation

At the age of 5–7 weeks, mice of each genotype were divided in two groups and fed with different diets for one year. The first group received a normal purified mouse diet containing 5% crude fat in the form of LCT, corresponding to 12% of metabolizable energy as calculated with Atwater factors (ssniff® EF R/M Control, ssniff Spezialdiäten GmbH, Soest, Germany). The second group was fed with a diet corresponding as well to 12% of total metabolizable energy. Here, 4.4% from a total of 5% fat was MCT (Ceres®MCT-oil, basis GmbH, Oberpfaffenhofen, Germany) while the remaining 0.6% was derived from soy bean oil to provide the required essential long-chain fatty acids. The content of essential long-chain fatty acids was calculated in accordance with the Nutrient Requirements of Laboratory Animals (Subcommittee on Laboratory Animal Nutrition, Committee on Animal Nutrition, Board on Agriculture, National Research Council). Both diets based on purified feed ingredients contained the same nutrient concentration as follows: 94.8% dry matter, 17.8% crude protein (N × 6.25), 5% crude fat, 5% crude fiber, 5.3% crude ash, 61.9% nitrogen free extract, 36.8% starch, 14.8% dextrin and 11% sugar. The detailed fatty acid composition of the diets was previously reported [20]. In both diets the carbohydrate and protein contents corresponded to 69% and 19% of metabolizable energy, respectively. All mouse groups received water ad libitum.

2.3. Cardiac magnetic resonance imaging and spectroscopy

Data were recorded on a Bruker Avance^{III} 9.4 Tesla Wide Bore (89 mm) nuclear magnetic resonance (MR) spectrometer operating at frequencies of 400.13 MHz for ^{1}H and 161.97 MHz for ^{31}P measurements as previously described [21]. Experiments were carried out using a Bruker microimaging unit (Mini 0.5) equipped with actively shielded gradient sets (capable of 1 T/m maximum gradient strength and 150 μs rise time at 100% gradient switching), a dual tunable ^{1}H/^{31}P 30-mm birdcage resonator, and Paravision 5.1 as operating software. The mice were anesthetized with 1.5% isoflurane and were kept at 37 °C. For functional analysis, high resolution images of mouse hearts were acquired using an ECG- and respiratory-triggered fast gradient echo cine sequences. A flip angle of 25°, echo time of 1.8 ms, and a repetition time of about 4 ms were used. The pixel size after zero filling was 117 × 117 μm^2 (field of view, 30 × 30 mm^2; matrix, 128 × 128; acquisition time per slice for one cine sequence, 1–2 min). Six to eight contiguous ventricular short axis slices (slice thickness 1 mm) were acquired to cover the entire heart.

Subsequently, cardiac high energy phosphates were analyzed using 2D ^{31}P chemical shift imaging (CSI). The slice used for spectroscopic imaging (6 mm) was placed mid-ventricular in short-axis orientation covering almost the entire heart from apex to the base. Fieldmap-based shimming (MAPSHIM) was carried out to optimize the field homogeneity in the region of interest. The 2D ^{31}P CSI data set was recorded with a sine-bell acquisition-weighted sequence to improve the spatial response function using the following parameters: flip angle, 45°; repetition time (TR), 250 ms; field of view, 30 × 30 mm^2; matrix 16 × 16 (voxel size ~ 20 μl); data points in the spectral domain, 1024; spectral width, 6510 Hz; slice selection with a 500-μs sinc3 pulse; acquisition time, 75 min [21]. An exponential filter of 20 Hz was applied in the spectroscopic direction and chemical shifts were referenced to the PCr resonance at −2.52 ppm. For quantification of myocardial PCr/ATP ratios, only voxels covering the free left ventricular wall were considered, since in both groups spectra of septal voxels were occasionally contaminated with ^{31}P signals originating from chamber blood as reflected by the appearance of 2,3-diphosphoglycerate (DPG) signals (data not shown).

2.4. Positron emission tomography (PET) imaging

F-18-fluordeoxyglucose (FDG, 10 MBq) in 100 μl 0.9% saline was injected intraperitoneally without anesthesia since this would have had effects on blood insulin and glucose levels. After 1 h of tracer distribution animals were anesthetized with isoflurane (1.5–2.0%) and placed on a heating pad to maintain the body temperature. PET list mode data was acquired for 15 min using the 32-module quadHIDAC scanner (Oxford Positron Systems, Weston-on-the-Green, UK) dedicated to small animal imaging. The scanner has an effective resolution of 0.7 mm (FWHM) in the transaxial and axial directions when using an iterative resolution recovery reconstruction algorithm. PET data were reconstructed into a single image volume for each mouse with a voxel size 0.4 × 0.4 × 0.4 mm^3. Quantification of segmental tracer uptake and volumes of the left ventricle was performed using in-house software programmed in MATLAB (The Mathworks) and C programming languages [22].

2.5. Tissue homogenates

Tissues were homogenized with Cellytic MT Buffer (Sigma-Aldrich, Steinheim, Germany) in the presence of 1 mg ml^{-1} protease inhibitors and centrifuged at 4 °C and 16,000 *g* for 10 min to pelletize any cell debris. The clear supernatant was immediately used for the enzyme assays or stored at −80 °C. Protein concentration of tissue homogenates was determined using the BSA method as previously described [23].

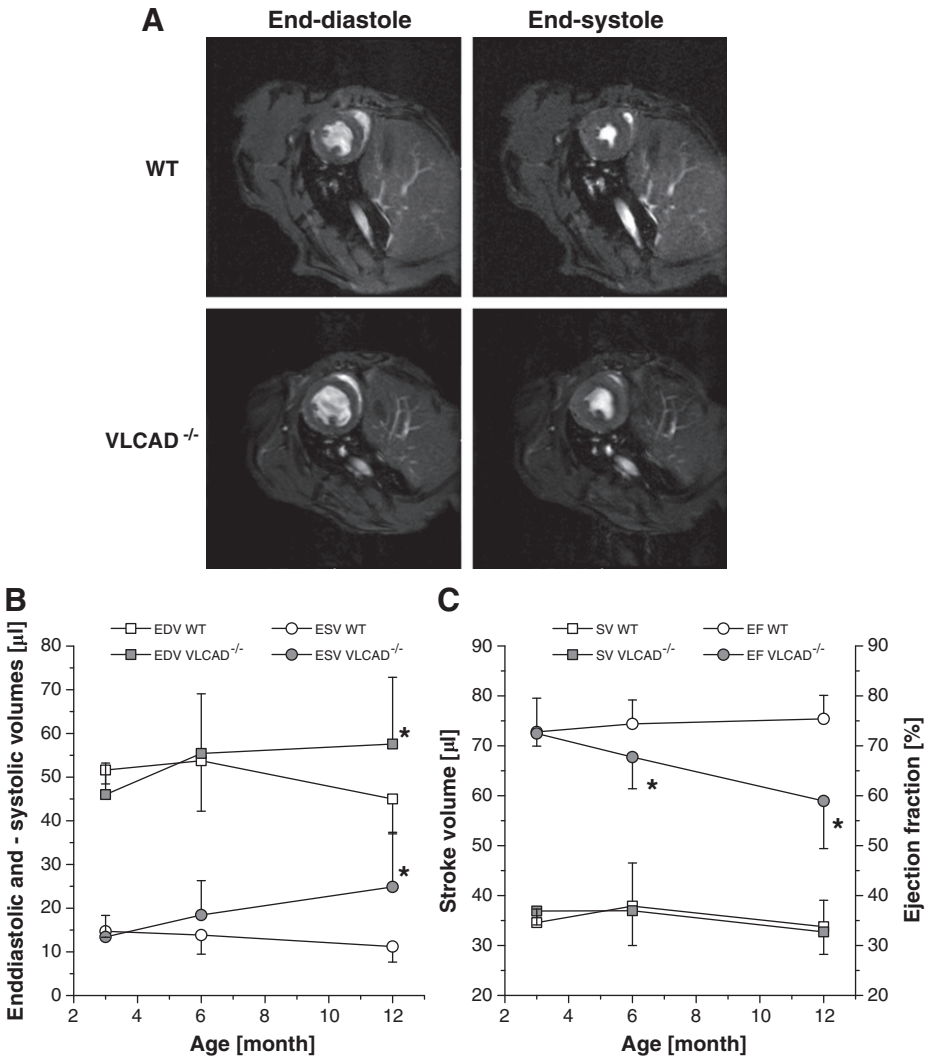

Fig. 1. Time course of cardiac function of WT and VLCAD$^{-/-}$ mice under control diet. A) Representative short-axis ^{1}H-MR images in end-diastole and end-systole of WT and VLCAD$^{-/-}$ mice at the age of 12 months. B) End-diastolic and end-systolic volumes at the age of 3, 6 and 12 months. C) Stroke volume and ejection fraction at the age of 3, 6 and 12 months. * indicates significant differences between WT and VLCAD$^{-/-}$ mice ($n = 10$–12).

2.6. Analysis of cardiac triacylglycerides (TAG), thiobarbituric acid reactive substances (TBARS), reduced glutathione (GSH) and protein carbonylation degree

Cardiac TAG were extracted from lyophilized tissue and measured as duplicates on an Infinite M200 Tecan (Crailsheim, Germany) plate reader as previously reported [14]. All assays were performed following the manufacturer's instructions. The measurement of TBARS was performed as previously described [13]. GSH was measured with the Glutathione Assay Kit (Cayman Chemical, Ann Arbor, USA). Measurement of protein carbonylation was performed with the Protein Carbonylation Assay Kit (Cayman Chemical, Ann Arbor, USA).

2.7. Measurement of pyruvate kinase (PK) activity, ketone bodies and lactate

PK activity was performed in duplicate using the Pyruvate Kinase Assay Kit (BioVision, Mountain View, USA) as recommended by the manufacturer's instruction. Ketone bodies were measured with a Precision Xceed blood sugar meter (Abbott, Wiesbaden, Germany). Measurement of lactate was performed using the Lactate Assay Kit (Sigma-Aldrich, Steinheim, Germany) following the manufacturer's instructions.

2.8. RT-PCR analysis

Total RNA from heart was isolated with the RNeasy mini kit (Qiagen, Hilden Germany). Forward and reverse primers were designed with the FastPCR program (R. Kalendar, Institute of Biotechnology, Helsinki). Gene function and primer sequences are reported in Supplemental Table 1. RT-PCR was performed in a single step procedure with the QuantiTect SYBR Green™ RT-PCR (Qiagen, Hilden, Germany) on an Applied Biosystems 7500 Real-Time PCR-System (Applied Biosystems, Foster City, CA, USA). β-Actin was used as reference gene.

2.9. Statistical analysis

MRI data are reported as mean values ± standard deviation (SD). All other data are presented as means ± standard error of the mean (SEM). *n* denotes the number of animals tested. Analysis for the significance of differences was performed using Student's t-tests for paired and unpaired data and Wilcoxon-Signed-Rank Test. To test the effects of the two variables, diet and genotype, two-way analysis of variance (ANOVA) with Bonferroni post-test was performed (GraphPad Prism 5, San Diego California USA). Differences were considered significant if $p < 0.05$.

3. Results

3.1. Progressive development of systolic dysfunction in VLCAD$^{-/-}$ mice

The long-term effects of a defective mFAO on cardiac function in VLCAD$^{-/-}$ mice were analyzed in WT and mutants under a normal diet at the age of 3, 6 and 12 months by cine ^{1}H MRI. Fig. 1A shows representative short-axis MRIs of one year old mice in end-diastole and end-systole (see also Supplemental Movies 1 and 2). At this age VLCAD$^{-/-}$ mice exhibited significantly increased end-diastolic and end-systolic volumes (EDV + ESV) resulting in a pronounced reduction of ejection fraction (EF) as compared to WT mice (58.9 ± 9.5% vs 75.4 ± 4.7%; $p < 0.01$; $n = 10$). This functional impairment occurred progressively (Fig. 1B + C), in that EF was already significantly reduced in VLCAD$^{-/-}$ mice at the age of 6 months and further worsened in 12 month-old mice. Nevertheless, stroke volume and thereby cardiac output remained unaffected (Fig. 1C). Planimetry of the myocardial walls revealed a mild transient hypertrophy in 6 month-old VLCAD$^{-/-}$ mice as compared to WT controls (end-diastolic wall thickness: 1.08 ± 0.07 vs 1.00 ± 0.07 mm; $p < 0.05$). However, these differences were not anymore observed in one year old mice, but VLCAD$^{-/-}$ mice displayed a significant reduction in systolic wall thickness (1.43 ± 0.23 vs 1.67 ± 0.15 mm; $p < 0.05$) indicative of systolic dysfunction.

3.2. Impaired myocardial energetics and glucose metabolism in 12 month-old VLCAD$^{-/-}$ mice

To analyze the metabolic state, we first measured myocardial energetics of mutants and littermates at the age of 12 months by 2D-^{31}P-CSI. Fig. 2A top shows representative ^{31}P-MR spectra extracted from full CSI data sets of WT and VLCAD$^{-/-}$ mice in correlation with the anatomical end-diastolic ^{1}H MR image. As can be seen, dilation of VLCAD$^{-/-}$ hearts (right) is accompanied by a marked decrease of cardiac phosphocreatine (PCr) levels. Averaging the high energy phosphate levels over posterior, lateral, and anterior walls revealed a significantly decreased PCr-to-ATP ratio (1.48 ± 0.29 vs. 2.01 ± 0.26; $p < 0.05$; Fig. 2B) over the entire left ventricle. The observed effects were caused by a drop in PCr levels since no differences in ATP levels were detected between the groups.

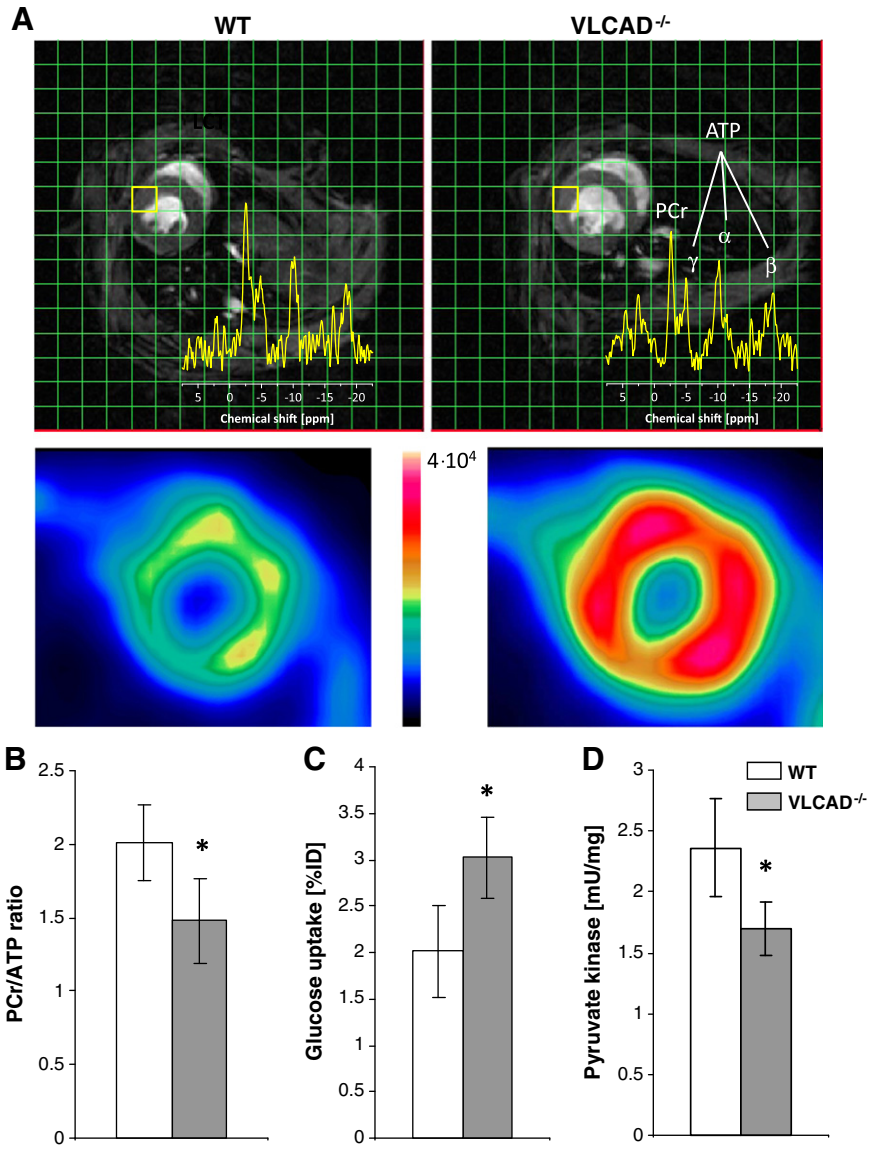

Fig. 2. Myocardial energetics and glucose metabolism in 12 month-old WT and VLCAD$^{-/-}$ mice. A) Representative short-axis ^{1}H-MR images in end-diastole and corresponding ^{31}P-MR spectra (top) as well as myocardial glucose uptake measured by FDG-PET (bottom) in WT and VLCAD$^{-/-}$ mice. B) PCr/ATP ratio quantified from in vivo by 2D-^{31}P-CSI datasets (averaged over the entire free wall of the left ventricle). C) Glucose uptake determined by in vivo FDG-PET. D) Pyruvate kinase activity measured in heart homogenate of WT and VLCAD$^{-/-}$ mice. All analyses were performed in 12 month-old mice. * indicates significant differences between WT and VLCAD$^{-/-}$ mice (n = 10–12).

In parallel experiments, we analyzed whether the imbalanced myocardial energy state in VLCAD$^{-/-}$ mice was also accompanied by alterations in cardiac substrate metabolism. FDG-PET as noninvasive measure of myocardial glucose uptake showed in mutants indeed a higher FDG uptake as compared to WT mice (3.02 ± 0.44 vs 2.01 ± 0.5% ID, Fig. 2A bottom + C). Surprisingly, this did not correspond to an increased pyruvate kinase (PK) activity which was found to be significantly lower in mutant hearts (1.70 ± 0.22 vs 2.36 ± 0.4 mU/mg, $p < 0.05$; Fig. 2D). Because of this metabolic decompensation we measured the expression of genes typically expressed in developing hearts and down-regulated in adult organs known as genes of the fetal gene program, namely *Acta1*, *MHCα*, *MHCβ* and *Glut4*. However, in failing heart these are again up-regulated to compensate for cardiac metabolic derangement [24]. Especially *Acta1* was markedly up-regulated in mutants as compared to WT (315.6 ± 5.7 vs 99.9 ± 1.2%; $p < 0.05$). In line with the decreased PK activity, *PDK4*, which is known to inhibit glucose oxidation, was significantly up-regulated in mutants (308.7 ± 9.4 vs 100 ± 3.8%; $p < 0.05$; $n = 10$; see also below), whereas the glucose transporter *Glut4* was strongly down-regulated (50.4 ± 12.4 vs 100.5 ± 18.3%; $p < 0.05$; $n = 10$; see also below). Of note, we found no evidence for an altered utilization of alternative substrates, such as ketone bodies or lactate, in VLCAD$^{-/-}$ mice under control diet (see below).

3.3. MCT diet does not prevent the gradual development of cardiomyopathy in VLCAD$^{-/-}$ mice

In the next step, we investigated whether a continuous MCT diet could counteract the observed phenotype. Surprisingly, this diet resulted in WT control mice in a significant reduction in EF as compared to untreated WT (69.41 ± 4.41 vs 75.40 ± 4.71%; $p < 0.05$; $n = 10$; Fig. 3B). Even more critically, in the mutants long-term MCT diet not only failed to attenuate cardiac dysfunction, but even aggravated the degree of cardiomyopathy as illustrated in representative long-axis MRIs in Fig. 3A. End-systolic images acquired after one year of diet clearly indicate the exacerbation of systolic dysfunction in VLCAD$^{-/-}$ mice fed with MCT (see also Supplemental Movies 3–6). Already after 6 months a reduction in systolic wall thickness was observed in VLCAD$^{-/-}$ mice fed with MCT compared to mice under control diet (1.47 ± 0.15 vs 1.62 ± 0.36 mm of WT; $p < 0.05$; Fig. 3C). In mutants treated with MCT for 12 months, EF was further reduced in comparison with VLCAD$^{-/-}$ mice under normal diet (52.35 ± 7.49 vs 58.95 ±9.54%; $p < 0.05$; $n = 10$; Fig. 3B). This functional impairment was accompanied by significantly reduced systolic and diastolic wall thicknesses (Fig. 3D). Additional cardiac parameters such as end-systolic and end-diastolic volumes given in Supplementary Table 1 further strengthened these findings.

3.4. Impairment of energy metabolism and reactivation of the fetal gene program

To gain insight into the underlying metabolic pathomechanisms, we analyzed heart homogenates for genes typically expressed during fetal development. Long-term supplementation with MCT for 12 months led VLCAD$^{-/-}$ mutants to a dramatic up-regulation of *Acta1* as compared to WT under the same dietary regimen (Fig. 4B) indicative of cardiac stress and accompanied by energy deficiency as shown by in vivo ^{31}P-CSI findings. Of note, this was not yet observed after 6 months of MCT diet, but interestingly at this point of time *Acta1* was significantly up-regulated in mutants under control diet — but to a substantial

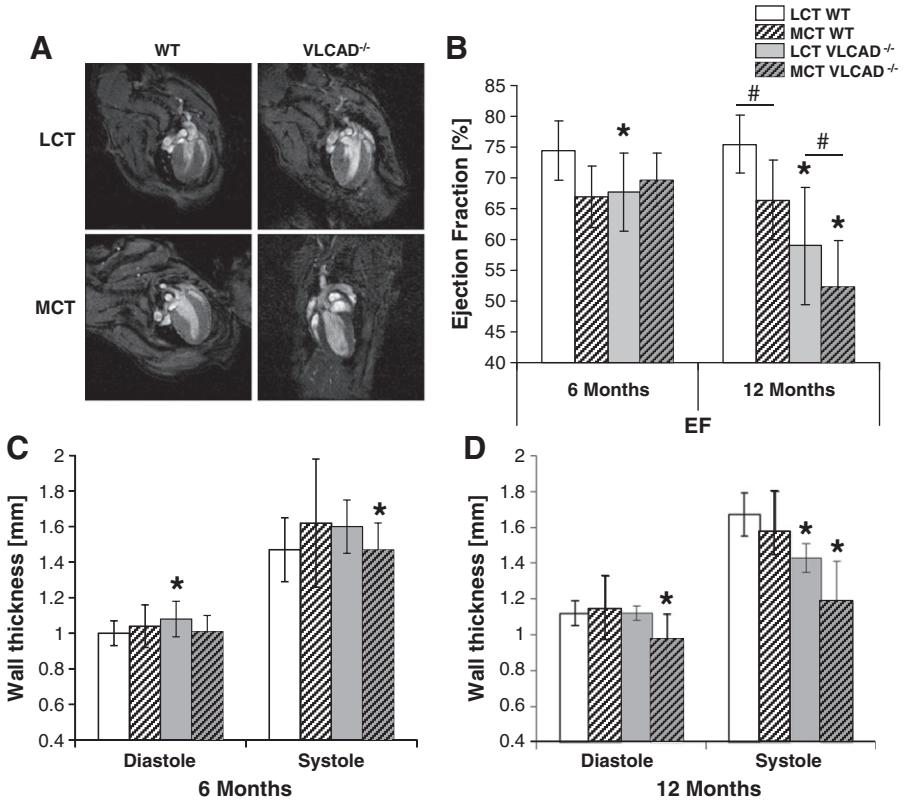

Fig. 3. Effect of a long-term MCT diet on cardiac function of WT and VLCAD$^{-/-}$ mice. A) Representative long-axis ^{1}H-MR images in end-systole of WT and VLCAD$^{-/-}$ mice under either control or MCT diet at the age of 12 months. B) Ejection fraction of WT and VLCAD$^{-/-}$ mice under control and MCT diet at the age of 6 and 12 months. C + D) Diastolic and systolic wall thickness in mice at the age of 6 and 12 months. * indicates significant differences between WT and VLCAD$^{-/-}$ mice within a diet group. # indicates significant differences between WT and VLCAD$^{-/-}$ mice under different dietary conditions as compared to control diet ($n = 10$–12).

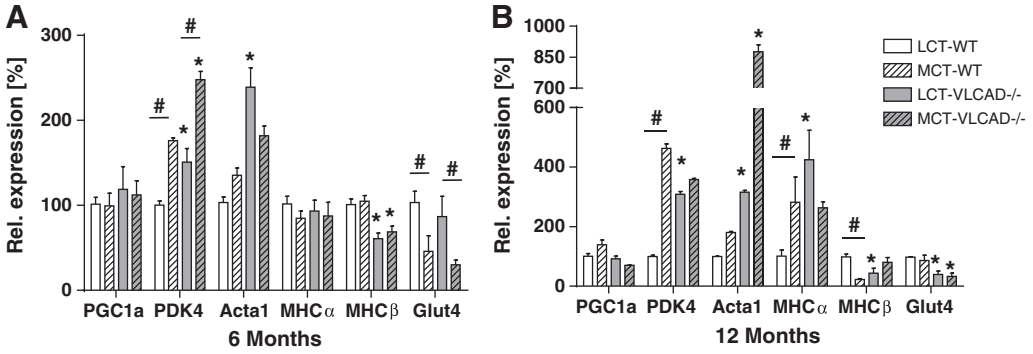

Fig. 4. Cardiac energy metabolism and reactivation of the fetal gene program in WT and VLCAD$^{-/-}$ mice under either control or MCT diet at the age of 6 A) and 12 B) months. Relative expression of *PGC1α*, *PDK4*, *Acta1*, *MHCα*, *MHCβ* and *Glut4* was performed by RT-PCR analysis. Values are expressed as % of WT mice ($n = 10–12$). * indicates significant differences between WT and VLCAD$^{-/-}$ mice within a diet group. # indicates significant differences between WT and VLCAD$^{-/-}$ mice under different dietary conditions as compared to control diet.

lower degree as compared to 12 months of MCT diet ($p < 0.05$; Fig. 4A + B). In parallel, the down-regulation of *Glut4* with a concomitant up-regulation of *PDK4* under MCT in both groups in mice at the age of 6 months (Fig. 4A), which persisted up to 12 months suggested an inhibition of glucose uptake and oxidation.

3.5. Alternative substrates under normal and MCT diet

Since supplementation of MCT is known to elevate circulating levels of ketone bodies (KB) which may be used as alternative substrates, we determined KB concentrations in the hearts of one year old mice. Fig. 5A shows no differences between WT and VLCAD$^{-/-}$ mice under normal diet. In contrast, as typical effect of MCT both genotypes under this dietary regimen displayed a markedly higher concentration of KB, whereas lactate concentration was affected neither by the genotype nor by the diet (Fig. 5A). In accordance to the increase in KB content, the expression of cardiac *Bdh1* and *Acat1* both critically involved in ketolysis was significantly up-regulated suggesting an enhanced use of KB for energy production under MCT diet in both genotypes ($p < 0.05$; Fig. 5B).

3.6. MCT diet induces cardiac lipid accumulation and oxidative stress

Finally, we investigated the effects of both diets on cardiac lipid homeostasis after one year [20]. Triglyceride (TAG) concentrations were found to be much higher in the hearts of mice under MCT diet (Fig. 6A). In particular, VLCAD$^{-/-}$ mice showed a significantly higher TAG content as compared to mutants under normal diet (74.01 ± 12.71 vs 44.73 ± 8.41 μmol/g; $p < 0.05$). In a similar manner, the concentration of thiobarbituric acid reactive substances (TBARS), end products in the degradation of lipid peroxides, was significantly increased in these mice with a two-fold higher TBARS content as compared to VLCAD$^{-/-}$ mice under normal diet (4.1 ± 1.0 vs 2.1 ± 0.6 μmol/g; $p < 0.05$; Fig. 6B). The content of reduced glutathione (GSH) was already significantly lower in mutants under normal diet, whereas MCT supplementation led to a further decrease of GSH in both genotypes (Fig. 6C). Likewise, tissue levels of carbonylated proteins were observed to be elevated in mutants under control diet, and MCT diet significantly enhanced oxidative protein carbonylation in both genotypes under MCT diet ($p < 0.05$; Fig. 6D).

Oxidative stress was also documented by the peculiar gene expression profiles of uncoupling proteins *UCP2* and *UCP3* (Fig. 6E–F) induced by increased circulating fatty acids as occurred in mice under MCT diet [20]. At the age of 6 months, when VLCAD$^{-/-}$ mice developed a transient hypertrophy under normal diet, a strong up-regulation of *UCP2* was observed, which has been described as compensatory mechanism to reduce the electrical potential across the inner mitochondrial membrane avoiding the production of superoxide radicals in the period prior to heart failure [25]. At that time also UCP3 was significantly up-regulated suggesting the presence of oxidative stress already at this age ($p < 0.05$; Fig. 6E). The expression of *UCP2* normalized in all groups at the age of 12 months as reported after heart failure, however, both genotypes fed with MCT further showed a significant up-regulation of *UCP3* expression ($p < 0.05$; Fig. 6F). This expression pattern of genes coding for UCP proteins strongly resembles the cardiac phenotype associated with diabetic disease [26]. In accordance to a previous report, *PPARα* which regulates the availability of fatty acids and the activity of FAO machinery was down-regulated in VLCAD$^{-/-}$ mice at the age of 6 and 12 months [9] (Fig. 6E–F).

4. Discussion

In this study we demonstrate for the first time that VLCAD-deficient mice develop progressive cardiac dysfunction without the trigger of

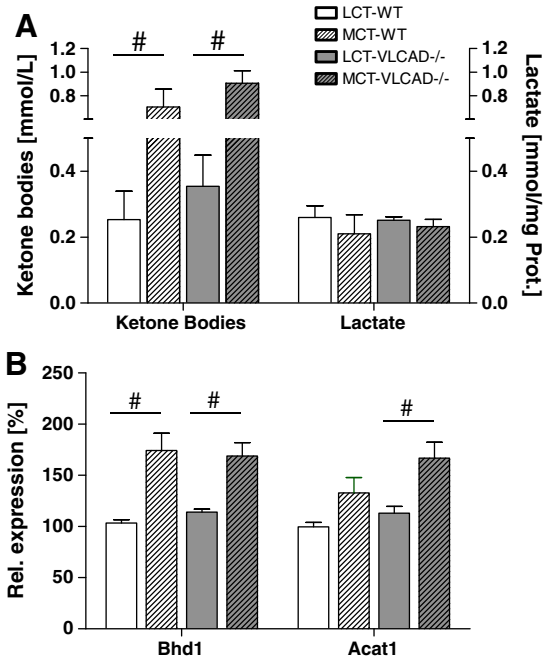

Fig. 5. Cardiac substrate concentrations and metabolism in WT and VLCAD$^{-/-}$ mice under either control or MCT diet. A) Ketone bodies and lactate concentration. B) Relative expression of *Bdh1* and *Acat1* analyzed by RT-PCR. Values are expressed as % of WT mice ($n = 10–12$). * indicates significant differences between WT and VLCAD$^{-/-}$ mice within a diet group. # indicates significant differences between WT and VLCAD$^{-/-}$ mice under different dietary conditions as compared to control diet.

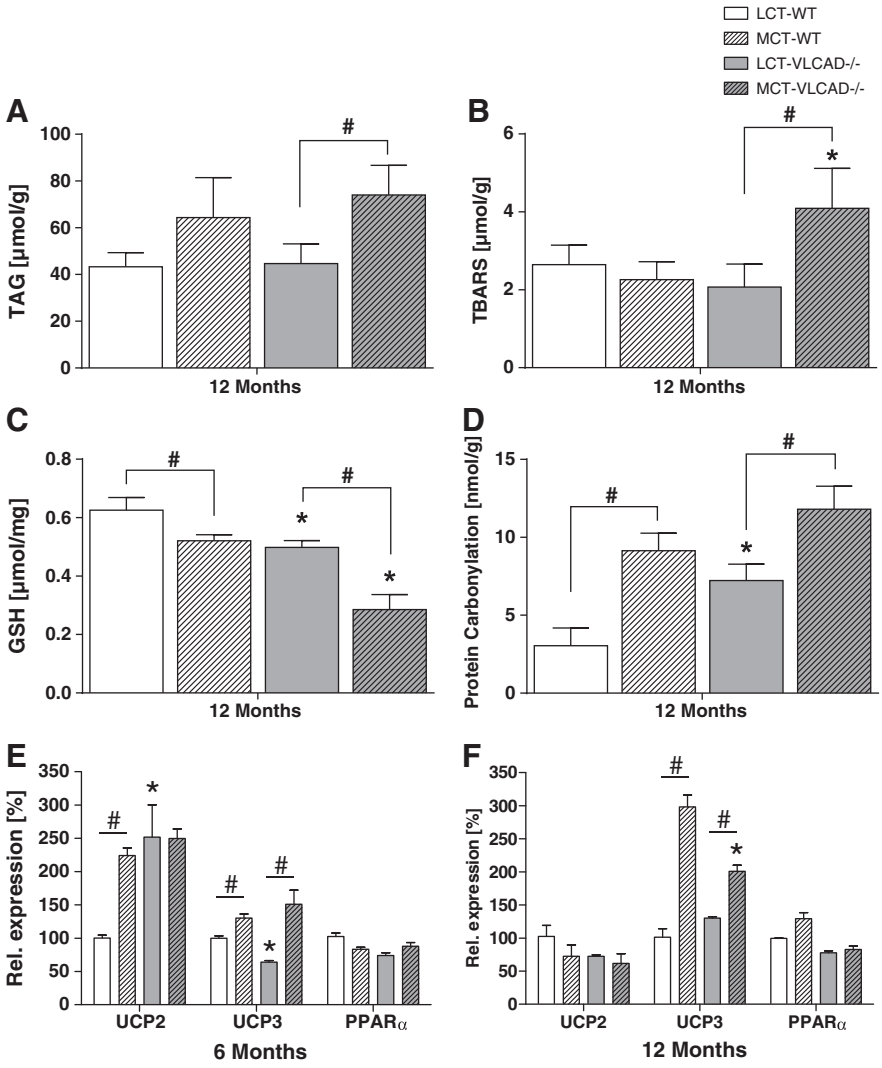

Fig. 6. Effect of an MCT diet on cardiac lipid accumulation and oxidative stress. Triglyceride A), TBARS B) accumulation, reduced glutathione C) and protein carbonylation content D) in mice fed either a control or an MCT diet at the age of 12 months. Relative expression of *UCP2*, *UCP3* and *PPARα* analyzed by RT-PCR in mice at E) 6 and F) 12 months ($n = 10$–12). * indicates significant differences between WT and VLCAD$^{-/-}$ mice within a diet group. # indicates significant differences between WT and VLCAD$^{-/-}$ mice under different dietary conditions as compared to control diet.

catabolic situations. VLCAD$^{-/-}$ mice suffer already under resting conditions a chronic and continuous energy deficiency leading to pronounced metabolic and functional cardiac decompensation over time. Although the benefit of MCT on metabolically deranged patients with acute cardiomyopathy has been proven in several clinical studies, we show that the long-term application of this diet in VLCAD$^{-/-}$ mice could not prevent the temporal development of cardiac dysfunction but even aggravated the cardiac phenotype to a diabetic form of dilated cardiomyopathy.

Since non-stressed young VLCAD$^{-/-}$ mice were described as asymptomatic [11,12,20] we initially hypothesized that an up-regulation of glucose oxidation together with an increase in oxidative capacity of long-chain acyl-CoA dehydrogenase (LCAD), a β-oxidation enzyme with overlapping substrate specificity, could compensate for lacking VLCAD oxidation capacity [15,27]. Indeed, glucose uptake in 12 month-old VLCAD$^{-/-}$ mice was increased as shown by FDG-PET analysis indicative of enhanced glucose flux. On the other hand, the reduction of pyruvate kinase activity with a concomitant up-regulation of PDK4 expression and a reduced expression of the gene coding for GLUT4 transporter suggest a down-regulation of the glucose oxidation pathway as also observed by Lei et al. in the failing dog heart [28,29]. In addition to that, VLCAD$^{-/-}$ mice display an inverse relationship between enhanced myocardial glucose uptake and a reduced PCr/ATP ratio similar to previous reports on cardiac substrate metabolism in hypertrophied hearts [30,31]. Since VLCAD$^{-/-}$ mice display an expression pattern of genes typically up-regulated in developing hearts and in adult hearts solely in cases of functional impairment and metabolic derangement [32] we hypothesize that despite enhanced glucose flux the overall cardiac energy production is impaired resulting in the development of cardiac dysfunction over time.

There is recent evidence that in mice with β-oxidation defects, under severe catabolic conditions the accumulation of triglycerides results in lipotoxicity, which contributes to the onset of arrhythmia and left ventricular dysfunction [18,33]. However, the present investigation was performed in the well-fed, resting state during which the mutants do accumulate neither cardiac TAG (Fig. 6A) nor acylcarnitines [34]. Therefore, lipotoxicity is unlikely to be the predominant mechanism in the development of cardiomyopathy in VLCAD$^{-/-}$ mice under a normal diet, in strong contrast to mice supplemented with an MCT diet. Here, lipotoxicity plays a key role as shown by TAG accumulation and lipid peroxides in form of TBARS, which clearly represent a link between oxidative stress and heart failure as their tissue levels inversely correlate with the ejection fraction [35,36]. Indeed, not only VLCAD$^{-/-}$ mice but also WT mice supplemented with a long-term MCT diet displayed a marked accumulation of TAG and oxidative stress accompanied by a

significant impairment of cardiac function. These findings corroborate our hypothesis of MCT-induced lipotoxicity when applied long-term during energetic steady state periods independent of the presence of a mitochondrial fatty acid β-oxidation defect. Similar to the reported data on the effects of MCT in the liver, the marked reduction of GSH accompanied by enhanced protein carbonylation underline the striking effect of MCT in promoting oxidative stress. These findings correlate with the marked expression of the *UCP3* gene observed in the hearts of WT and VLCAD$^{-/-}$ mice after long-term MCT supplementation (Fig. 6F). Although we did not measure enzyme activities it is reported that the uncoupling capacity of *UCP3* is activated by lipid peroxides, by decreasing mitochondrial ROS production and reducing their downstream detrimental effects [37]. The expression profiles of the uncoupling proteins *UCP2* and *UCP3* support the fact that oxidative stress further aggravates cardiac dysfunction under MCT diet. At the age of 6 months under both dietary regimens, VLCAD$^{-/-}$ mice displayed higher expression of *UCP2*. This up-regulation has been reported in the period prior to heart failure to meet the production of superoxide radicals at complex I of the mitochondrial respiratory chain [25,38]. In contrast, in 12 month-old mutants under both diets the expression of *UCP2* is down-regulated as reported in failing hearts [39] while mutants at the same age upon MCT strongly express *UCP3* resembling the expression profile of diabetic hearts [26].

MCT supplementation results in a high content of circulating medium-chain fatty acids in the blood, which may be easily absorbed by the organs. Furthermore, MCT are highly ketogenic which is reflected by increased ketone body production and the enhanced expression of genes coding for enzymes of the ketolytic pathway (Fig. 5) suggesting an increased utilization of these substrates in the hearts of both genotypes. However, higher ketone body concentrations increase the acetyl CoA/CoA and NADH/NAD ratios within the mitochondria contributing to the inhibition of the pyruvate dehydrogenase complex by up-regulation of PDK4 [40,41]. This effect is amplified by the high free fatty acid content in blood of VLCAD$^{-/-}$ mice [20] which also impacts on metabolism by inhibiting glucose uptake and oxidation [42]. Although MCT quickly supply the organism with metabolizable substrates, in the long-run glucose oxidation will be inhibited and medium-chain fatty acids will be converted into long-chain fatty acids aggravating the metabolic state of VLCAD$^{-/-}$ mice [20,43].

During metabolic derangement, however, the supplementation with MCT has been proven to be effective especially in the treatment of the acute cardiomyopathy and in the prevention of rhabdomyolysis [6,7,43,44]. In isolated cases Roe et al. [45]. reported on the positive effect of triheptanoin.

In summary, we demonstrate that under well-fed conditions VLCAD$^{-/-}$ mice gradually develop cardiac dysfunction due to chronic energy deficiency that is not triggered by catabolic derangements. We also demonstrate that dietary interventions affect cardiac energy production pathways. MCT cannot effectively supply VLCAD-deficient mice hearts with sufficient energy long-term. Moreover, MCT-induced lipotoxicity during energy steady state periods aggravates the cardiac phenotype degenerating into diabetic-like dilated cardiomyopathy. Similar but milder effects may also appear in asymptomatic patients if supplemented continuously and long-term with an MCT diet when not needed, although MCT is able to fully reverse cardiomyopathy if applied during catabolic situations [6]. The results of this study also show that cardiac MRI and MRS may be excellent tools to assess minor changes in cardiac function and energetics in patients with β-oxidation defects to initiate adequate preventive therapy.

Supplementary data to this article can be found online at http://dx.doi.org/10.1016/j.bbadis.2014.02.001.

Acknowledgements

We thank Mrs Sarah Köster for help with image analysis and Dr. Christoph Jacoby for help in MRI analysis. All authors read and approved the final manuscript. The authors have no conflict of interest to disclose. ST designed and conducted the research, and wrote the manuscript; UF performed MR analysis and draft the manuscript; SV and MS performed PET analysis; MS contributed to data collection; US drafted the manuscript and had primary responsibility for final content. This study was supported by grants from the Deutsche Forschungsgemeinschaft [SFB 612 TP-B9 to US and TP-Z2 to UF], from the Forschungskommission of the Medical Faculty of Heinrich Heine University, and from the Interdisziplinäres Zentrum für Klinische Forschung (IZKF), University of Muenster, Germany (Core Unit PIX to SH).

References

[1] A.W. Strauss, C.K. Powell, D.E. Hale, M.M. Anderson, A. Ahuja, J.C. Brackett, H.F. Sims, Molecular basis of human mitochondrial very-long-chain acyl-CoA dehydrogenase deficiency causing cardiomyopathy and sudden death in childhood, Proc. Natl. Acad. Sci. U. S. A. 92 (1995) 10496–10500.
[2] U. Spiekerkoetter, B. Sun, T. Zytkovicz, R. Wanders, A.W. Strauss, U. Wendel, MS/MS-based newborn and family screening detects asymptomatic patients with very-long-chain acyl-CoA dehydrogenase deficiency, J. Pediatr. 143 (2003) 335–342.
[3] J.M. Saudubray, D. Martin, P. de Lonlay, G. Touati, F. Poggi-Travert, D. Bonnet, P. Jouvet, M. Boutron, A. Slama, C. Vianey-Saban, J.P. Bonnefont, D. Rabier, P. Kamoun, M. Brivet, Recognition and management of fatty acid oxidation defects: a series of 107 patients, J. Inherit. Metab. Dis. 22 (1999) 488–502.
[4] G.L. Arnold, J. Van Hove, D. Freedenberg, A. Strauss, N. Longo, B. Burton, C. Garganta, C. Ficicioglu, S. Cederbaum, C. Harding, R.G. Boles, D. Matern, P. Chakraborty, A. Feigenbaum, A Delphi clinical practice protocol for the management of very long chain acyl-CoA dehydrogenase deficiency, Mol. Genet. Metab. 96 (2009) 85–90.
[5] U. Spiekerkoetter, J. Bastin, M. Gillingham, A. Morris, F. Wijburg, B. Wilcken, Current issues regarding treatment of mitochondrial fatty acid oxidation disorders, J. Inherit. Metab. Dis. 33 (2010) 555–561.
[6] M.C. Brown-Harrison, M.A. Nada, H. Sprecher, C. Vianey-Saban, J. Farquhar Jr., A.C. Gilladoga, C.R. Roe, Very long chain acyl-CoA dehydrogenase deficiency: successful treatment of acute cardiomyopathy, Biochem. Mol. Med. 58 (1996) 59–65.
[7] M.A. Pervaiz, F. Kendal, M. Hegde, R.H. Singh, MCT oil-based diet reverses hypertrophic cardiomyopathy in a patient with very long chain acyl-coA dehydrogenase deficiency, Indian J. Hum. Genet. 17 (2011) 29–32.
[8] V.J. Exil, R.L. Roberts, H. Sims, J.E. McLaughlin, R.A. Malkin, C.D. Gardner, G. Ni, J.N. Rottman, A.W. Strauss, Very-long-chain acyl-coenzyme a dehydrogenase deficiency in mice, Circ. Res. 93 (2003) 448–455.
[9] V.J. Exil, C.D. Gardner, J.N. Rottman, H. Sims, B. Bartelds, Z. Khuchua, R. Sindhal, G. Ni, A.W. Strauss, Abnormal mitochondrial bioenergetics and heart rate dysfunction in mice lacking very-long-chain acyl-CoA dehydrogenase, Am. J. Physiol. Heart Circ. Physiol. 290 (2006) H1289–H1297.
[10] E.S. Goetzman, L. Tian, P.A. Wood, Differential induction of genes in liver and brown adipose tissue regulated by peroxisome proliferator-activated receptor-alpha during fasting and cold exposure in acyl-CoA dehydrogenase-deficient mice, Mol. Genet. Metab. 84 (2005) 39–47.
[11] U. Spiekerkoetter, J. Ruiter, C. Tokunaga, U. Wendel, E. Mayatepek, F.A. Wijburg, A.W. Strauss, R.J. Wanders, Evidence for impaired gluconeogenesis in very long-chain acyl-CoA dehydrogenase-deficient mice, hormone and metabolic research, Hormon- und Stoffwechselforschung Horm. Metab. 38 (2006) 625–630.
[12] U. Spiekerkoetter, C. Tokunaga, U. Wendel, E. Mayatepek, L. Ijlst, F.M. Vaz, N. van Vlies, H. Overmars, M. Duran, F.A. Wijburg, R.J. Wanders, A.W. Strauss, Tissue carnitine homeostasis in very-long-chain acyl-CoA dehydrogenase-deficient mice, Pediatr. Res. 57 (2005) 760–764.
[13] S. Tucci, S. Primassin, U. Spiekerkoetter, Fasting-induced oxidative stress in very long chain acyl-CoA dehydrogenase-deficient mice, FEBS J. 277 (2010) 4699–4708.
[14] S. Tucci, S. Primassin, F. Ter Veld, U. Spiekerkoetter, Medium-chain triglycerides impair lipid metabolism and induce hepatic steatosis in very long-chain acyl-CoA dehydrogenase (VLCAD)-deficient mice, Mol. Genet. Metab. 101 (2010) 40–47.
[15] M. Chegary, H. Brinke, J.P. Ruiter, F.A. Wijburg, M.S. Stoll, P.E. Minkler, M. van Weeghel, H. Schulz, C.L. Hoppel, R.J. Wanders, S.M. Houten, Mitochondrial long chain fatty acid beta-oxidation in man and mouse, Biochim. Biophys. Acta 1791 (2009) 806–815.
[16] K.B. Cox, D.A. Hamm, D.S. Millington, D. Matern, J. Vockley, P. Rinaldo, C.A. Pinkert, W.J. Rhead, J.R. Lindsey, P.A. Wood, Gestational, pathologic and biochemical differences between very long-chain acyl-CoA dehydrogenase deficiency and long-chain acyl-CoA dehydrogenase deficiency in the mouse, Hum. Mol. Genet. 10 (2001) 2069–2077.
[17] A.A. Werdich, F. Baudenbacher, I. Dzhura, L.H. Jeyakumar, P.J. Kannankeril, S. Fleischer, A. LeGrone, D. Milatovic, M. Aschner, A.W. Strauss, M.E. Anderson, V.J. Exil, Polymorphic ventricular tachycardia and abnormal Ca^{2+} handling in very-long-chain acyl-CoA dehydrogenase null mice, Am. J. Physiol. Heart Circ. Physiol. 292 (2007) H2202–H2211.
[18] R. Gelinas, J. Thompson-Legault, B. Bouchard, C. Daneault, A. Mansour, M.A. Gillis, G. Charron, V. Gavino, F. Labarthe, C. Des Rosiers, Prolonged QT interval and lipid alterations beyond beta-oxidation in very long-chain acyl-CoA dehydrogenase null mouse hearts, Am. J. Physiol. Heart Circ. Physiol. 301 (2011) H813–H823.
[19] K.B. Cox, J. Liu, L. Tian, S. Barnes, Q. Yang, P.A. Wood, Cardiac hypertrophy in mice with long-chain acyl-CoA dehydrogenase or very long-chain acyl-CoA dehydrogenase deficiency, Lab. Invest. 89 (2009) 1348–1354.

[20] S. Tucci, U. Flogel, M. Sturm, E. Borsch, U. Spiekerkoetter, Disrupted fat distribution and composition due to medium-chain triglycerides in mice with a beta-oxidation defect, Am. J. Clin. Nutr. 94 (2011) 439–449.
[21] U. Flogel, C. Jacoby, A. Godecke, J. Schrader, In vivo 2D mapping of impaired murine cardiac energetics in NO-induced heart failure, Magn. Reson. Med. 57 (2007) 50–58.
[22] L. Stegger, K.P. Schafers, U. Flogel, L. Livieratos, S. Hermann, C. Jacoby, P. Keul, E.M. Conway, O. Schober, J. Schrader, B. Levkau, M. Schafers, Monitoring left ventricular dilation in mice with PET, J. Nucl. Med. 46 (2005) 1516–1521.
[23] M.M. Bradford, A rapid and sensitive method for the quantitation of microgram quantities of protein utilizing the principle of protein–dye binding, Anal. Biochem. 72 (1976) 248–254.
[24] K. Kuwahara, T. Nishikimi, K. Nakao, Transcriptional regulation of the fetal cardiac gene program, J. Pharmacol. Sci. 119 (2012) 198–203.
[25] S.S. Liu, Generating, partitioning, targeting and functioning of superoxide in mitochondria, Biosci. Rep. 17 (1997) 259–272.
[26] K.R. Laskowski, R.R. Russell 3rd, Uncoupling proteins in heart failure, Curr. Heart Fail. Rep. 5 (2008) 75–79.
[27] S. Tucci, D. Herebian, M. Sturm, A. Seibt, U. Spiekerkoetter, Tissue-specific strategies of the very-long chain acyl-CoA dehydrogenase-deficient (VLCAD$^{-/-}$) mouse to compensate a defective fatty acid beta-oxidation, PLoS One 7 (2012) e45429.
[28] B. Lei, V. Lionetti, M.E. Young, M.P. Chandler, C. d'Agostino, E. Kang, M. Altarejos, K. Matsuo, T.H. Hintze, W.C. Stanley, F.A. Recchia, Paradoxical downregulation of the glucose oxidation pathway despite enhanced flux in severe heart failure, J. Mol. Cell. Cardiol. 36 (2004) 567–576.
[29] P. Razeghi, M.E. Young, J. Ying, C. Depre, I.P. Uray, J. Kolesar, G.L. Shipley, C.S. Moravec, P.J. Davies, O.H. Frazier, H. Taegtmeyer, Downregulation of metabolic gene expression in failing human heart before and after mechanical unloading, Cardiology 97 (2002) 203–209.
[30] S. Boudina, S. Sena, B.T. O'Neill, P. Tathireddy, M.E. Young, E.D. Abel, Reduced mitochondrial oxidative capacity and increased mitochondrial uncoupling impair myocardial energetics in obesity, Circulation 112 (2005) 2686–2695.
[31] L. Nascimben, J.S. Ingwall, B.H. Lorell, I. Pinz, V. Schultz, K. Tornheim, R. Tian, Mechanisms for increased glycolysis in the hypertrophied rat heart, Hypertension 44 (2004) 662–667.
[32] H. Taegtmeyer, S. Sen, D. Vela, Return to the fetal gene program: a suggested metabolic link to gene expression in the heart, Ann. N. Y. Acad. Sci. 1188 (2010) 191–198.
[33] A.J. Bakermans, T.R. Geraedts, M. van Weeghel, S. Denis, M. Joao Ferraz, J.M. Aerts, J. Aten, K. Nicolay, S.M. Houten, J.J. Prompers, Fasting-induced myocardial lipid accumulation in long-chain acyl-CoA dehydrogenase knockout mice is accompanied by impaired left ventricular function, Circ. Cardiovasc. Imaging 4 (2011) 558–565.
[34] S. Tucci, S. Pearson, D. Herebian, U. Spiekerkoetter, Long-term dietary effects on substrate selection and muscle fiber type in very-long-chain acyl-CoA dehydrogenase deficient (VLCAD(−/−)) mice, Biochim. Biophys. Acta 1832 (2013) 509–516.
[35] K. Nakamura, K.F. Kusano, H. Matsubara, Y. Nakamura, A. Miura, N. Nishii, K. Banba, S. Nagase, K. Miyaji, H. Morita, H. Saito, T. Emori, T. Ohe, Relationship between oxidative stress and systolic dysfunction in patients with hypertrophic cardiomyopathy, J. Card. Fail. 11 (2005) 117–123.
[36] F. Sam, D.L. Kerstetter, D.R. Pimental, S. Mulukutla, A. Tabaee, M.R. Bristow, W.S. Colucci, D.B. Sawyer, Increased reactive oxygen species production and functional alterations in antioxidant enzymes in human failing myocardium, J. Card. Fail. 11 (2005) 473–480.
[37] M. Nabben, J. Hoeks, Mitochondrial uncoupling protein 3 and its role in cardiac- and skeletal muscle metabolism, Physiol. Behav. 94 (2008) 259–269.
[38] M.N. Sack, Mitochondrial depolarization and the role of uncoupling proteins in ischemia tolerance, Cardiovasc. Res. 72 (2006) 210–219.
[39] H. Taegtmeyer, P. Razeghi, M.E. Young, Mitochondrial proteins in hypertrophy and atrophy: a transcript analysis in rat heart, Clin. Exp. Pharmacol. Physiol. 29 (2002) 346–350.
[40] P.W. Felts, O.B. Crofford, C.R. Park, Effect of infused ketone bodies on glucose utilization in the dog, J. Clin. Invest. 43 (1964) 638–646.
[41] P.J. Randle, P.B. Garland, C.N. Hales, E.A. Newsholme, The glucose fatty-acid cycle. Its role in insulin sensitivity and the metabolic disturbances of diabetes mellitus, Lancet 1 (1963) 785–789.
[42] R. Vettor, R. Fabris, R. Serra, A.M. Lombardi, C. Tonello, M. Granzotto, M.O. Marzolo, M.O. Carruba, D. Ricquier, G. Federspil, E. Nisoli, Changes in FAT/CD36, UCP2, UCP3 and GLUT4 gene expression during lipid infusion in rat skeletal and heart muscle, Int. J. Obes. Relat. Metab. Disord. 26 (2002) 838–847.
[43] S. Primassin, S. Tucci, D. Herebian, A. Seibt, L. Hoffmann, F. ter Veld, U. Spiekerkoetter, Pre-exercise medium-chain triglyceride application prevents acylcarnitine accumulation in skeletal muscle from very-long-chain acyl-CoA-dehydrogenase-deficient mice, J. Inherit. Metab. Dis. 33 (2010) 237–246.
[44] U. Spiekerkoetter, Effects of a fat load and exercise on asymptomatic VLCAD deficiency, J. Inherit. Metab. Dis. 30 (2007) 405.
[45] C.R. Roe, L. Sweetman, D.S. Roe, F. David, H. Brunengraber, Treatment of cardiomyopathy and rhabdomyolysis in long-chain fat oxidation disorders using an anaplerotic odd-chain triglyceride, J. Clin. Invest. 110 (2002) 259–269.